

Synthesis of flower-like WS_2 by chemical vapor deposition

Jin-Zi Ding(丁金姿), Wei Ren(任卫), Ai-Ling Feng(冯爱玲), Yao Wang(王垚), Hao-Sen Qiao(乔浩森), Yu-Xin Jia(贾煜欣), Shuang-Xiong Ma(马双雄), and Bo-Yu Zhang(张博宇)

Citation: Chin. Phys. B, 2021, 30 (**12**): 126201. DOI: 10.1088/1674-1056/ac0524
Journal homepage: http://cpb.iphy.ac.cn; http://iopscience.iop.org/cpb

What follows is a list of articles you may be interested in

Effect of nitrogen gas flow and growth temperature on extension of GaN layer on Si

Jian-Kai Xu(徐健凯), Li-Juan Jiang(姜丽娟), Qian Wang(王茜), Quan Wang(王权), Hong-Ling Xiao(肖红领), Chun Feng(冯春), Wei Li(李巍), and Xiao-Liang Wang(王晓亮)

Chin. Phys. B, 2021, 30 (**11**): 118101. DOI: 10.1088/1674-1056/abff30

Direct growth of graphene films without catalyst on flexible glass substrates by PECVD

Rui-Xia Miao(苗瑞霞), Chen-He Zhao(赵晨鹤), Shao-Qing Wang(王少青), Wei Ren(任卫), Yong-Feng Li(李永锋), Ti-Kang Shu(束体康), and Ben Yang(杨奔)

Chin. Phys. B, 2021, 30 (**9**): 098101. DOI: 10.1088/1674-1056/abeeec

Effect of hydrogen content on dielectric strength of the silicon nitride film deposited by ICP-CVD

Yudong Zhang(张玉栋), Jiale Tang(唐家乐), Yongjie Hu(胡永杰), Jie Yuan(袁杰), Lulu Guan(管路路), Xingyu Li(李星雨), Hushan Cui(崔虎山), Guanghui Ding(丁光辉), Xinying Shi(石新颖), Kaidong Xu(许开东), and Shiwei Zhuang(庄仕伟)

Chin. Phys. B, 2021, 30 (**4**): 048103. DOI: 10.1088/1674-1056/abea82

A MOVPE method for improving InGaN growth quality by pre-introducing TMIn

Zi-Kun Cao(曹子坤), De-Gang Zhao(赵德刚), Jing Yang(杨静), Jian-Jun Zhu(朱建军), Feng Liang(梁锋), and Zong-Shun Liu(刘宗顺)

Chin. Phys. B, 2021, 30 (**1**): 018103. DOI: 10.1088/1674-1056/abb801

Synthesis mechanism of nanoporous Sn_3O_4 nanosheets by hydrothermal process without any additives

Zhao Jun-Hua, Tan Rui-Qin, Yang Ye, Xu Wei, Li Jia, Shen Wen-Feng, Wu Guo-Qiang, Zhu You-Liang, Yang Xu-Feng, Song Wei-Jie

Chin. Phys. B, 2015, 24 (**6**): 066202. DOI: 10.1088/1674-1056/24/6/066202

Synthesis of flower-like WS_2 by chemical vapor deposition*

Jin-Zi Ding(丁金姿)[1], Wei Ren(任卫)[2,†], Ai-Ling Feng(冯爱玲)[1,‡], Yao Wang(王垚)[2], Hao-Sen Qiao(乔浩森)[2], Yu-Xin Jia(贾煜欣)[2], Shuang-Xiong Ma(马双雄)[2], and Bo-Yu Zhang(张博宇)[2]

[1] *Institute of Physics & Optoelectronics Technology, Baoji University of Arts and Sciences, Baoji* 721016, *China*
[2] *School of Science, Xi'an University of Posts & Telecommunications, Xi'an* 710121, *China*

(Received 9 February 2021; revised manuscript received 10 May 2021; accepted manuscript online 26 May 2021)

Flower-like tungsten disulfide (WS_2) with a diameter of 5–10 μm is prepared by chemical vapor deposition (CVD). Scanning electron microscopy (SEM), energy dispersive spectrometer (EDS), Raman spectroscopy, and ultraviolet-visible (UV-vis) spectroscopy are used to characterize its morphological and optical properties, and its growth mechanism is discussed. The key factors for the formation of flower-like WS_2 are determined. Firstly, the cooling process causes the generation of nucleation dislocations, and then the "leaf" growth of flower-like WS_2 is achieved by increasing the temperature.

Keywords: flower-like WS_2, chemical vapor deposition (CVD), optical property, growth mechanism

PACS: 62.23.Kn, 81.15.Gh, 68.55.−a, 78.20.Ci **DOI:** 10.1088/1674-1056/ac0524

1. Introduction

Tungsten disulfide (WS_2) is a transition metal chalcogenide compound composed of some layers, in which each layer is formed by periodic S–W–S atomic structure. The atoms in each layer are bonded by strong covalent bonds, and the layers are bonded by van der Waals forces.[1,2] WS_2 exhibits excellent optical, electrical and chemical sensing properties, making it promising for a wide range of applications like catalysis, laser modulation, batteries, and lubricants.[3–5] Such excellent properties of WS_2 are closely related to the number of layers and the geometrical morphology. As a result, the processing control over the synthesis of WS_2 materials to yield materials with better geometrical morphologies and good physical/chemical properties has attracted widespread attention.

WS_2 with various geometrical morphologies have been reported by different synthesis procedures. The hydrothermal method and chemical vapor deposition (CVD) method are among these techniques. For instance, Cao *et al.*[6] reported four different morphologies of WS_2 by the hydrothermal method (nanoparticles, nanorods, nanosheets, and nanofibers). Besides, numerous studies have been devoted to the CVD method to prepare the single-layer or multilayer WS_2 films in the horizontal direction. In recent years, CVD has been employed to prepare WS_2 with different morphologies. For example, Sharma *et al.*[7] used CVD to synthesize independent dendritic and fibrous WS_2 on gold foil. In 2019, Ahmadi *et al.*[8] obtained WS_2 nanosheets in the vertical direction by the low-temperature CVD method. However, the synthesis of flower-like WS_2 is rarely reported by using the atmospheric pressure CVD. Due to its large specific surface area, the flower-like WS_2 may be used as a promising catalyst in hydrogen evolution reaction catalysis.

In this study, flower-like WS_2 are grown by using the CVD method, and the morphological formation mechanism of WS_2 is revealed.

2. Experimental details

WO_3 powder (Aladdin, particle size $<$ 200 nm, purity 99.9%) and sulphur (S) powder (ZhongNuo Advanced Material, particle size $<$ 100 mesh, purity 99.9%) were used as raw materials. The substrates were made of two pieces of quartz plates (size 1×1 cm^2, thickness 500 μm). These substrates were sonicated in acetone, alcohol, and deionized water for 15 min to yield the clean surfaces.

The samples were grown in a tube furnace (model OTF-1200X, HF Ke Jing company). Firstly, put 0.09 g of WO_3 nano-powder in 10 ml ethanol to form a tungsten alcohol suspension, and keep it under magnetic stirring for 10 min to make the particles evenly distributed. Before the reaction, a droplet (10 μL) of the suspension was taken by a pipette and dropped on a clean quartz substrate (bottom substrate). After evaporation of ethanol, a relatively uniform-distributed WO_3 powder was obtained on the substrate surface. Next, another quartz substrate (top) with the same size was placed face-down just on the bottom substrate dripped with WO_3 suspension to form a sandwich structure. To stabilize the reaction gas flow, a one-end-closed quartz tube with a smaller diameter (diameter of 1.5 cm) was horizontally put inside the large quartz tube (diameter of 2.4 cm). S powder (600 g) was placed in

*Project supported by the Joint Research Funds of Department of Science & Technology of Shaanxi Province and Northwestern Polytechnical University (Grant No. 2020GXLH-Z-029).

†Corresponding author. E-mail: renwei@xupt.edu.cn
‡Corresponding author. E-mail: ailing@mail.xjtu.edu.cn

© 2021 Chinese Physical Society and IOP Publishing Ltd

the bottom of the sealed end of the small quartz tube. The sandwich-structured substrates were also carefully placed inside the small quartz tube at a position of 12 cm away from the S powder. The sandwich-structured system also provides an additional gas-flow-stabilizing environment for the growth of WS_2. Finally, the position of the smaller quartz tube containing the precursor and the substrates were adjusted to the center of the larger quartz tube of the furnace to allow the growth of 2D materials. The detailed experimental diagram is provided in Fig. 1(a). Before reaching the reaction temperature, the substrate of the sandwich structure was 4 cm from the center of the heating zone, and the S powder was 16 cm from the center of the heating zone (Fig. 1(b)(1)). Afterwards, the furnace was pumped to the low pressure of 10 Pa, and then purged at the atmospheric pressure with 100 sccm argon gas. These steps were repeated three times to allow a roughly cleaning of the furnace pipe. The experimental reaction process was carried out under an argon pressure of 50 sccm. After the preparation work was done, the heating program of the tube furnace was started. It should be noted that before reaching the preset growth temperature, the sandwich-type substrate was located at 4 cm away from the heating zone center. This method can avoid the chemical reaction of the reactants in advance (the temperature of the WO_3 powder is several degrees lower to the preset growth temperature in order to avoid WO_3 evaporation). After heating the furnace to the preset temperature of 850 °C, pushed the large quartz tube 4 cm to the left in order to ensure that the sandwich substrate structure was accurately placed to the center of the heating zone (condition 1: push tube). The position of the small quartz tube is shown in Fig. 1(b)(2)). Afterwards, a large amount of S powder and WO_3 source started to be evaporated and the redox reaction started to take place. The reaction can be summarized as below:

$$2WO_3 + 7S \rightarrow 2WS_2 + 3SO_2. \quad (1)$$

Subsequently, the temperature was lowered to 800 °C (condition 2: cooling process), and then increased to 850 °C at a rate of 10 °C per minute (condition 3: heating process), and reacted for 10 min until the temperature naturally dropped to room temperature. Finally, the samples were taken out of the quartz tube for subsequent characterization.

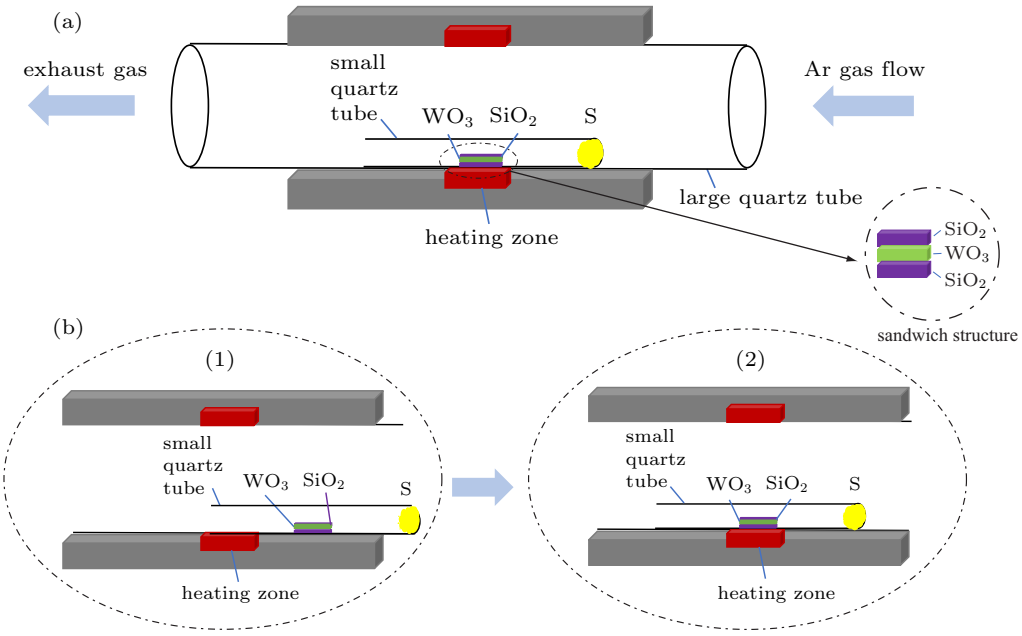


Fig. 1. (a) A diagram of the experimental device used for the synthesis of the flower-like WS_2 in a single-temperature zone furnace; (b) a schematic diagram showing the position change of the small quartz tube during the growth process.

The morphologies of the flower-like WS_2 materials were viewed by scanning electron microscopy (SEM, Hitachi FlexSEM 1000). The surface compositions were analyzed by energy dispersive spectrometer (EDS). Raman spectroscopy (Raman, Finder Vista, Zolix) in a back-scattering configuration (20 MW output power, 532 nm wavelength incidence light as the excitation source) was used to determine the bonding in WS_2 materials. The optical properties of the samples were studied by ultraviolet-visible spectrophotometry (UV-Vis, UV-3600 plus, Shimadzu, Japan).

3. Results and discussion

3.1. Morphology and structure

SEM images of the flower-like WS_2 products are presented in Fig. 2. Here, several aggregated flower-like WS_2 were obtained by adjusting the growth parameters. Since the bottom substrate contains more WO_3, the nucleation points are denser. In the growth period of 10 minutes, WO_3 on the bottom substrate reacts with a continuous stream of S vapor, and finally gathers and connects the flower-like WS_2 into dense clusters. In the top substrate, the formation of more single

flower-like WS_2 is due to the gap between the top substrate and the bottom one, which makes WO_3 at the bottom evaporate at high temperature and combine with S vapor to form a nucleation point on the top substrate, thus generates more single flower-like WS_2. Among them, the size of single flower-like WS_2 is about 5–10 μm. In Fig. 2(d), due to the different WO_3 content supplied by the bottom substrate, different morphologies of WS_2 like layers, pyramids, flowers, and flower-on-pyramids were formed. The single flower-like or sheet-like WS_2 prepared by hydrothermal method has the largest size of 5 μm,[9,10] but the size of the single flower-like WS_2 prepared by the CVD can reach 10 μm, and the single petal is larger. The flower-like WS_2 assembled from these petals has a larger specific surface area. This experiment also explored the influence of growth time and growth temperature on the preparation of flower-like WS_2, and the SEM image is shown in Fig. S1. The experimental results are shown in Table 1.

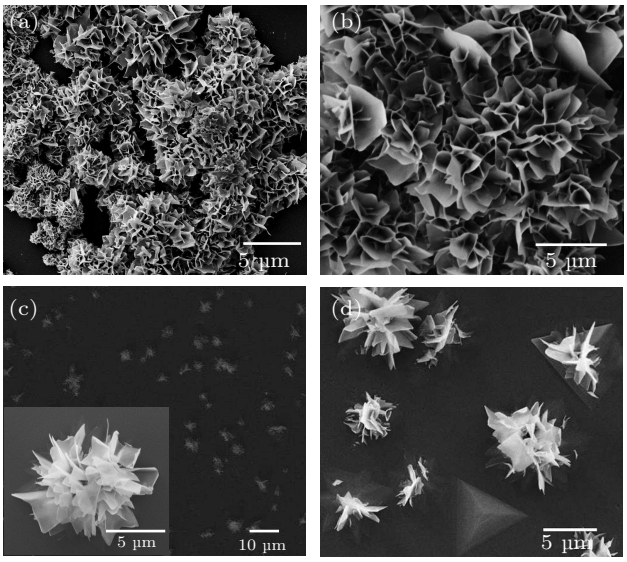


Fig. 2. SEM images of flower-like WS_2: (a), (b) images of the bottom substrate and (c), (d) images of the top substrate.

EDS energy spectrum analysis was performed on the red cross in the SEM image of the flower-like structure of the top and bottom substrates (Figs. 3(a) and 3(b)), only W and S signals were recorded, and the O signal was extremely weak. Basically, it can be concluded that WS_2 with a flower-like structure was formed. The element mapping analysis of the top and bottom substrates is shown in Figs. 4 and 5. The test location is also located in the SEM images in Figs. 3(a) and 3(b). Figure 4 shows the element distribution of a single flower-shaped WS_2. Figure 5 shows that the flower-like WS_2 under the bottom is relatively evenly distributed on the quartz substrate, and the W and S elements are densely distributed in the center of the flower.

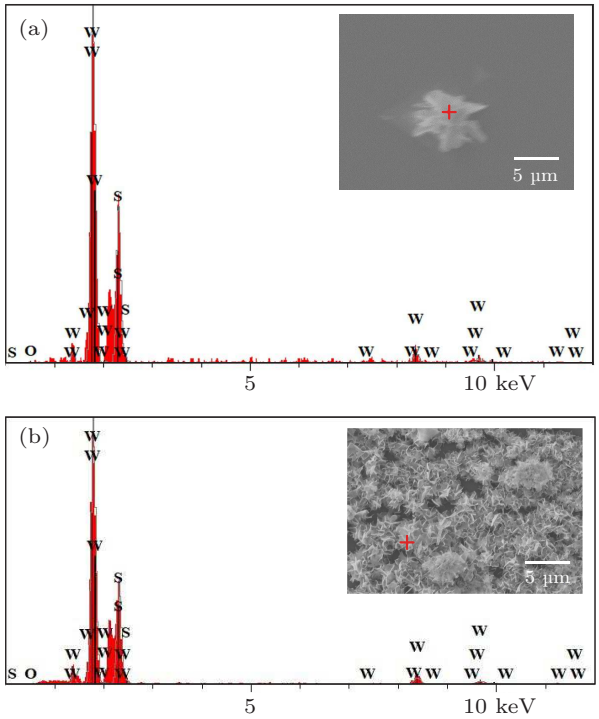


Fig. 3. EDS spectrum of flower-like WS_2: (a) the top substrate; (b) the bottom substrate.

Table 1. Summary of flower-like WS_2 prepared under different growth conditions.

Variable	Growth conditions	Sizes	Shape or morphology
Growth time	10 min	5–10 μm	Sparse flower-like structure
	20 min	The flower-like structure of WS_2 has obvious drop marks, and only some small flake-like structures remain	A small amount of lamellar structure
Growth temperature	850 °C	5–10 μm	Sparse flower-like structure
	900 °C	5–15 μm	Flower-like cluster structure

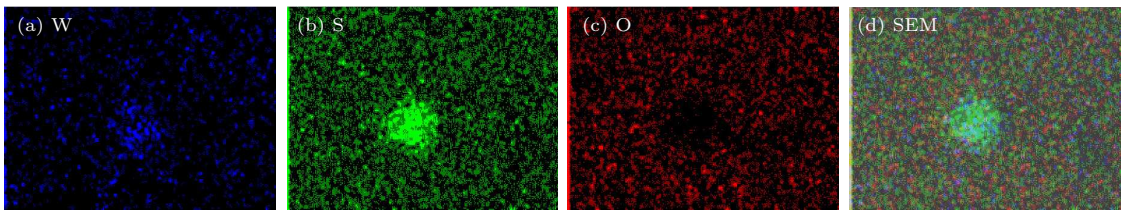


Fig. 4. EDS mapping diagram of flower-like WS_2 on top substrate: (a)–(c) elemental distributions of W, S, and O; (d) mixed diagram.

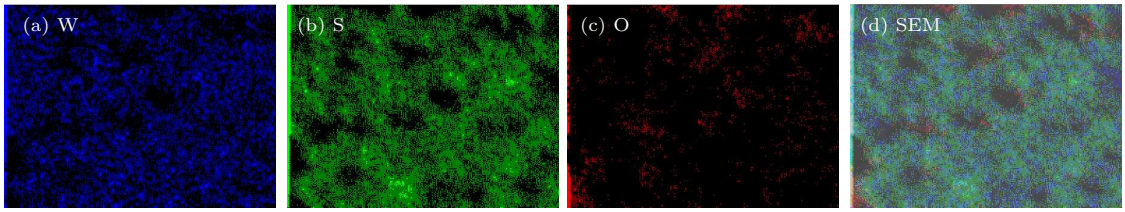


Fig. 5. EDS mapping diagram of flower-like WS_2 on bottom substrate: (a)–(c) elemental distributions of W, S, and O; (d) mixed diagram.

3.2. Optical properties of flower-like WS_2

To identify whether the flower-like structured material was made of WS_2, a 532 nm laser was used for Raman spectroscopy excitation. As shown in Fig. 6, two strong peaks were noticed at 348 cm^{-1} and 420 cm^{-1} and attributed to the E^1_{2g} and A_{1g} modes of WS_2, respectively. The peak positions were consistent with the previous reports.[8]

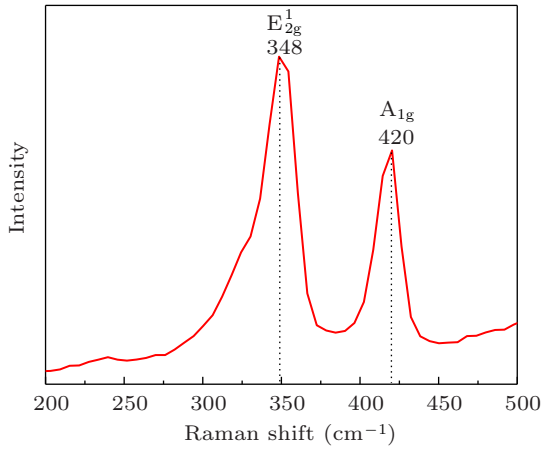


Fig. 6. Raman spectrum of flower-like WS_2 excited by 532 nm laser.

The UV-Vis absorption spectrum of the sample with flower-like WS_2 is illustrated in Fig. 7(a). The absorption wavelength belonged to the visible light range of 450–650 nm. A total of three peaks were observed and labeled as A (640 nm), B (532 nm), and C (463 nm). The A and B were characterized as the absorption peaks caused by the direct transition of point K from the valence band to the conduction band in the Brillouin zone.[11] Two peaks were formed when the spin orbits of the valence band split. The two absorption peaks were essentially identified as exciton peaks.[12] The peak C was associated with the optical transition between the valence state and density of states in the conduction band.[13]

The Tauc formula was utilized to calculate the optical energy band-gap (E_g) of the flower-like WS_2 [14]

$$(\alpha h\nu)^n = A(h\nu E_g), \tag{2}$$

where α, h, ν and A are the absorption coefficient, Planck's constant, frequency and a constant, respectively.

In general, $n = 2$ was employed to calculate the direct band-gap, and $n = 0.5$ was used to calculate the indirect band gap.[15] By drawing the relationship between $(\alpha h\nu)^n$ and $h\nu$, the linear part of the curve was used to extrapolate the optical energy band-gap. The flower-like WS_2 curves were obtained at $n = 2$. As can be seen, a linear part was noticed in the curve at $n = 2$ (Fig. 7(b)). The optical band gap of flower-like WS_2 was about 1.67 eV.

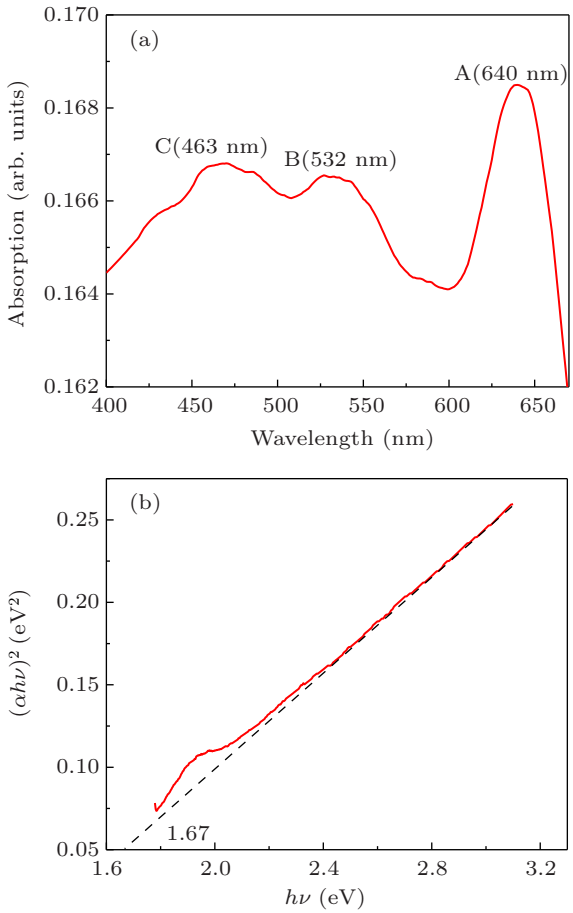


Fig. 7. (a) UV-Vis absorption spectrum of WS_2; (b) calculated Tauc diagram.

3.3. Key steps of forming flower-like WS_2

Compared with Fig. 2(a), the WS_2 structure in Fig. 2(d) is sparsely distributed. This is because the volatilization of the tungsten alcohol suspension dropped on the substrate surface led to incompletely distributed WO_3 powder, yielding different WO_3 contents in each nucleation point. Hence, appropriate amounts of WO_3 were required for sufficient reaction and guaranteed residual WO_3 was not left on the lower substrate. Appropriate amounts of WO_3 were mandatory to the formation of flower-like WS_2. After pushing in the small quartz

tube, WO_3 and S powder was quickly and sufficiently sublimated and reacted. During this procedure, both WO_3 and S powders were in a state of supersaturation, thereby increasing the initial nucleation rate and forming defects, especially dislocations. According to the layer-by-layer and dislocation-driven growth model, a tapered WS_2 film was quickly formed (Fig. 2(d)).[16,17] In addition to different WO_3 contents at each nucleation core, some flower-like structures were found to directly grow on top of the pyramidal WS_2 base, suggesting the consequent growth of the 'flower' on 'pyramid' structure.

Table 2. Main experimental conditions of 3 verification experiments.

Experiment No.	Push tube	Cooling process	Heating process	Reaction time
1	Yes	No	No	17 min
2	No	Yes	No	15 min
3	No	Yes	Yes	10 min

According to the experimental results, we can firstly determine that the prerequisite for the formation of flower-like WS_2 includes sufficient S powder content and an appropriate amount of WO_3. Secondly, it is speculated that the growth mechanism of flower-like WS_2 is mainly caused by the cooling process to cause the generation of nucleation dislocations, and then the "leaf" growth of flower-like WS_2 is achieved by increasing the temperature. In this part, in order to further reveal the evolution of the morphological structure of WS_2, three experiments with different processing procedures were designed (see Table 2 for the main experimental conditions without changing the other conditions). The specific processing steps of the experiments have been described in the Experimental section. Experiment 1 was designed to reveal the effects of pushing the quartz tube without temperature variation. Experiment 2 was to reveal the effects of the cooling process. Experiment 3 was to reveal the total effects of the cooling plus heating process on the WS_2 structures. The cooling process spent about 2 min, the heating process spent about 5 min, and the stable growth time was 10 min. To ensure the comparability of these experiments, the growth time of the three experiments were adjusted correspondingly, as shown in Table 1.

Figure 8 exhibits the samples' surface morphology of these experiments. Based on Fig. 8, the key feature of forming flower-like WS_2 is to firstly reduce the growth temperature from 850 °C to the predetermined 800 °C, then rapidly increase it to 850 °C, and finally keep stable temperature for 10 minutes. And the WS_2 growth can be divided into three phases: 1) cooling process; 2) heating process; and 3) stable growth. The cooling process will cause the newly formed triangle WS_2 surface to quickly produce large number of defects/dislocations with different directions. The consequent prompt heating process costs the low-temperature-induced defects/dislocation no time to be repaired. In the stable growth step, the low-temperature-induced defects become new nucleation sites so that large number of WS_2 flakes grow up along different angles to the substrate with sufficient reaction source. In Fig. 8(a) where the growth temperature is 850 °C, only planar triangle structures are seen. This phenomenon indicates that the triangle edges are active sites for material growth. The WS_2 can only grow at the layer-by-layer mode. This explains the finding of layers and pyramids in Fig. 2(d). In Fig. 8(b) where the sample growth temperature firstly rises to 850 °C and then decreases to 800 °C for 15 min, there finds many layered triangular WS_2 on the substrate surface, and many flake clusters grow on the layered triangular WS_2. Possibly due to the low growth temperature, the growth speed of WS_2 flakes is slow, and the sizes of these flake clusters are generally small. In Fig. 8(c) where the sample growth temperature firstly rises to 850 °C, decreases to 800 °C, then rises to 850 °C again (it spends about 5 min for the temperature rising to 850 °C), and finally keeps the temperature stable for 10 min. Due to the higher growth temperature, WS_2 forms larger flakes. Since there is no bedding for the tube pushing step, the nucleation points are randomly distributed, and most of them form nanosheets of about 1 μm, and the flower-like structure is not obvious. Therefore, pushing the tube is only a step to optimize the flower-like structure of WS_2, and the temperature variation is the key to determining the flower-like morphology of WS_2.

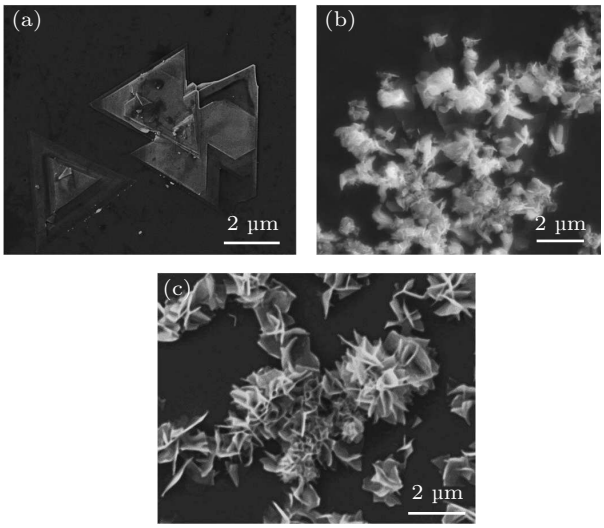


Fig. 8. SEM images of WS_2 samples obtained in three verification experiments. (a) Experiment 1. (b) Experiment 2. (c) Experiment 3.

4. Conclusions

Flower-like WS_2 with diameters of 5 to 10 μm were successfully formed through a simple atmospheric pressure CVD method. The experimental process was simple, low-cost, and required no doping of other elements. The flower-like WS_2 exhibited a wide range of visible light absorption property and was a promising catalyst in hydrogen evolution reaction catalysis. The main growth mode of WS_2 at 850 °C is at a planar layer-by-layer mode. When the growth temperature decreases from 850 °C to 800 °C, the defects/dislocations are induced on

top of the initially formed WS_2 layers and thereby WS_2 flakes can grow out of the horizontal plane and form the morphology of flower.

References

[1] Tenne R, Margulis L, Genut M and Hodes G 1992 *Nature* **360** 444

[2] Ramakrishna Matte H S S, Gomathi A, Manna A K, Late D J, Datta R, Pati S K and Rao C N R 2010 *Angew. Chem. Int. Ed.* **49** 4059

[3] Ma X L, Zhang R J, An C H, Wu S, Hu X D and Liu J 2019 *Chin. Phys. B* **28** 37803

[4] Cai Y, Li W, Feng Y, Zhao J S, Bai G, Xu J and Li J Z 2020 *Chin. Phys. B* **29** 110701

[5] Wang X, Li L, Li J P and Wang Y G 2017 *Chin. Phys. B* **26** 44203

[6] Cao S X, Liu T M, Hussain S, Zeng W, Peng X H and Pan F S 2014 *Mater. Lett.* **129** 205

[7] Sharma S, Jaisi B P, Sharma K P, Araby M I, Kalita G and Tanemura M 2018 *Phys. Status Solidi A* **215** 1700566

[8] Ahmadi A, Shoushtari M Z and Farbod M 2019 *Journal of Materials Science: Materials in Electronics* **30** 6342

[9] Cao S X, Zhao C, Peng L L and Han T 2016 *Journal of Materials Science: Materials in Electronics* **27** 3821

[10] Piao M X, Chu J, Wang X, Chi Y, Zhang H, Li C L, Shi H F and Joo M K 2018 *Nanotechnology* **29** 025705

[11] Bromley R A, Murray R B and Yoffe A D 1972 *J. Phys. C: Solid State Phys.* **5** 759

[12] Ross J S, Wu S F, Yu H Y, Ghimire N J, Jones A M, Aivazian G, Yan J Q, Mandrus D G, Xiao D, Yao W and Xu X D 2013 *Nat. Commun.* **4** 1474

[13] Mattheiss L F 1973 *Phys. Rev. B* **8** 3719

[14] Zirak M, Zhao M, Moradlou O, Samadi M, Sarikhani N, Wang Q, Zhang H L and Moshfegh A Z 2015 *Solar Energy Materials and Solar Cells* **141** 260

[15] Zirak M, Akhavan O, Moradlou O, Nien Y T and Moshfegh A Z 2014 *J. Alloys Compd.* **590** 507

[16] Sarma P V, Patil P D, Barman P K, Kini R N and Shaijumon M M 2016 *RSC Adv.* **6** 376

[17] Kumar P and Balakrishnan V 2018 *Appl. Surf. Sci.* **436** 846